Journal of Power Sources 189 (2009) 561–565

Contents lists available at ScienceDirect

Journal of Power Sources

journal homepage: www.elsevier.com/locate/jpowsour

Short communication

Electrochemistry of $LiMn_2O_4$ epitaxial films deposited on various single crystal substrates

Noriyuki Sonoyama[a,*], Kosuke Iwase[a], Hironori Takatsuka[a], Tadaaki Matsumura[b], Nobuyuki Imanishi[b], Yasuo Takeda[b], Ryoji Kanno[c]

[a] Department of Materials Science and Engineering, Nagoya Institute of Technology, Gokiso-cyo, Showa-ku, Nagoya 466-8555, Japan
[b] Department of Chemistry, Mie University, 1577 Kurimamachiyacho, Tsu, Mie 514-8507, Japan
[c] Department of Electronic Chemistry, Tokyo Institute of Technology, 4259 Nagatuta-cyo, Midori-ku, Yokohama 226-8502, Japan

ARTICLE INFO

Article history:
Received 30 July 2008
Received in revised form 3 October 2008
Accepted 5 October 2008
Available online 21 October 2008

Keywords:
Epitaxial film
$LiMn_2O_4$
Substrate effect
Absorption spectrum during lithium intercalation

ABSTRACT

$LiMn_2O_4$ epitaxial thin films were synthesized on $SrTiO_3$:Nb(1 1 1) and Al_2O_3(0 0 1) single crystal substrates by pulsed laser deposition (PLD) method and the electrochemical properties were discussed comparing with that of amorphous $LiMn_2O_4$ film on polycrystalline Au substrate. $LiMn_2O_4$ epitaxial film showed only a single plateau in charge–discharge curves and a single redox peak at the corresponding voltage of cyclic voltammograms. This phenomenon seems to originate from the effect of the epitaxy: the film is directly connected with the substrate by the chemical bond and this connection would suppress the phase transition of $Li_xMn_2O_4$ film during lithium (de-)intercalation. The discharge voltage of $LiMn_2O_4$ epitaxial film on $SrTiO_3$ was lower than that of $LiMn_2O_4$ film on Al_2O_3. This lowered discharge voltage may be caused by the electronic interaction between $LiMn_2O_4$ film and $SrTiO_3$:Nb n-type semiconductor substrate.

We also attempted to measure the absorption spectrum change of $LiMn_2O_4$ epitaxial film on Al_2O_3 during the lithium (de-)intercalation. The absorption spectrum of $LiMn_2O_4$ hardly changed during charging and discharging. This suggests the *d* orbital of Mn does not concern the 4 V region redox of $LiMn_2O_4$.

1. Introduction

Recently many of interests in lithium ion battery are devoted to rising its current density for the application of lithium battery to the electric vehicle and the middle scale power storage system. One of the effective methods for increasing current density of battery is diminishing the particle size of electrode material to nm level. The most successful example of this method is $LiFePO_4$ [1,2]. On the other hand, this method has limiting size for some materials. Honma et al. [3] reported that $LiCoO_2$ with nm order particle size loses its flat plateau in discharge curve.

The other approach to obtain the higher current density in lithium battery is acceleration of the electrode surface reaction. The lithium intercalation process at the electrode surface is known to be the rate limiting process [4] and its reaction mechanism is very complicated. This complex has made the surface reaction rate improvement difficult. Recently, many investigators have attempted the analysis or *in situ* detection of electrode surface products called solid electrolyte interface (SEI) [5–9] to determine the surface reaction mechanism during the lithium intercalation.

Epitaxial thin films of cathode materials, developed by Kanno et al. [10–12], are suitable electrodes for *in situ* X-ray reflectivity and surface diffraction measurements those are appropriate for proving the surface reaction mechanism. The characteristics of cathode epitaxial films are as follows: (1) surface roughness is very low (few nano meters), (2) effect of grain boundary is small, and (3) the orientation of the material can be controlled by the epitaxy. These characteristics of epitaxial films would be also favorable for the high rate intercalation. For the achievement of this purpose, optimization of the substrate materials is indispensable, because the substrate is directly connected with the films by the chemical bond and the interaction between the epitaxial films and substrates would be very strong.

In this paper, we evaporated $LiMn_2O_4$ on three kinds of substrates, polycrystalline Au, n-type semiconductor Nb-doped $SrTiO_3$ single crystal, and insulator Al_2O_3 single crystal. Electrochemical properties of these films were appreciated and the effect of substrates is discussed. On the basis of the electrochemical measurement techniques for thin films on the insulator substrate

* Corresponding author. Tel.: +81 52 735 7243; fax: +81 52 735 7243.
E-mail address: sonoyama@nitech.ac.jp (N. Sonoyama).

0378-7753/$ – see front matter © 2008 Elsevier B.V. All rights reserved.
doi:10.1016/j.jpowsour.2008.10.037

developed in this study, the absorption spectra of $LiMn_2O_4$ epitaxial films on Al_2O_3 substrate were measured during the lithium (de-)intercalation to investigate the electric structural change of $LiMn_2O_4$.

2. Experimental

$LiMn_2O_4$ films were grown using a KrF excimer laser with a wavelength of 248 nm and a pulsed laser deposition apparatus, PLD 3000 PVD Products, Inc. The substrates used were polycrystalline Au, single crystals of 1 1 1 orientated 0.5% Nb-doped $SrTiO_3$ (STO(1 1 1)), and 0 0 1 orientated Al_2O_3 (Al_2O_3(0 0 1)) substrate with the size of 10 mm × 10 mm × 0.5 mm. The substrates were annealed at 1000 °C before use. The targets of the PLD process were synthesized by sintering a mixture of starting materials, LiOH and MnO_x, at 900 °C for 24 h. The target had an excess lithium composition Li/Mn = 0.6 to compensate a lithium loss during the PLD process. Synthesis of thin film using PLD system was carried out under the optimized condition as previously reported [12]. The synthesis of WO_3 thin film on Al_2O_3(0 0 1) substrate was carried out using a PLD system (Ozawa Kagaku Inc., Japan). Light source was Q-switch Nd:YAG laser with a wavelength of 262 nm. The synthesis condition was 650 °C of substrate temperature, 30 Pa O_2 atmosphere for 0.5 h, and the distance between the target and the substrates was 7 cm. Thin-film X-ray diffraction data were recorded by a thin-film X-ray diffractometer (Rigaku ATX-G) or a powder X-ray diffractometer (Rigaku RAD-C) with Cu Kα radiation. The orientation of the epitaxial films was characterized both by the out-of-plane and in-plane techniques. For the electric contact to thin film deposited on the insulator substrate, Au was evaporated on all edges of thin films with 2-mm width. The charge–discharge characteristics of the epitaxial films were examined using a cell with lithium metal as an anode. The potential and current were controlled by a potentio-galvanostat (Hokuto HA-501) and a function generator (Hokuto HB-105). The electrolyte was ethylene carbonate–diethyl carbonate with a molar ratio of 3:7 as a solvent with a supporting electrolyte of 1 M $LiPF_6$. The charge–discharge current was 1 μA, otherwise noted. The ac conductivity was measured with a frequency-response analyzer (Solatron 1260) over a frequency range 10^{-1} to 10^7 Hz.

3. Results and discussion

3.1. Synthesis and characterization of the epitaxial films

Fig. 1(a) and (c) is the X-ray diffraction patterns of the out-of-plane measurements for $LiMn_2O_4$ films on the STO(1 1 1) and the Al_2O_3(0 0 1) substrates. These films showed the diffraction lines, 1 1 1, 2 2 2, 3 3 3, and 4 4 4, which indicates $LiMn_2O_4$ 1 1 1 orientation on both of STO(1 1 1) and Al_2O_3(0 0 1) substrates. The in-plane X-ray diffraction measurements along 0 1 $\bar{1}$ of STO and 1 0 0 of Al_2O_3 showed 2 $\bar{2}$ 0 and 4 $\bar{4}$ 0 reflections as were shown in Fig. 1(b) and (d).

For $LiMn_2O_4$ thin film evaporated on polycrystalline Au substrate, no reflection except for Au substrate was observed. We have discriminated that this result means the formation of amorphous $LiMn_2O_4$ film on Au surface on the basis that electrochemical property of this film, mentioned below, agreed well with that of a typical $LiMn_2O_4$ bulk electrode.

In the previous paper, we have reported that the thickness of $LiMn_2O_4$ epitaxial film on STO(1 1 1) substrate synthesized under the similar condition was 7–8 nm [12]. $LiMn_2O_4$ films on Al_2O_3, STO and Au substrates synthesized in this study would have similar extent of thickness.

3.2. Electrochemical property

The charge–discharge curves and cyclic voltammograms (CV) for $LiMn_2O_4$ film on polycrystalline Au substrate ($LiMn_2O_4$/Au) are shown in Fig. 2. The shapes of charge–discharge curves and CV curve are similar to those of bulk $LiMn_2O_4$: two plateaus were observed in the 4 V region. In CV curves, two peaks were obtained at the corresponding voltage. These CV peak positions of $LiMn_2O_4$/Au film agreed well with reports by other groups for $LiMn_2O_4$ films synthesized by PLD method [13–15]. The peak separation of CV peaks was summarized in Table 1. The peak separation values were small compared with bulk $LiMn_2O_4$ electrode even at the much faster scan rate. This means charge transfer rate at the $LiMn_2O_4$ thin film synthesized by PLD method is much faster than that for $LiMn_2O_4$ bulk electrode. This fast charge transfer at the thin film synthesized using the PLD method was also reported by other

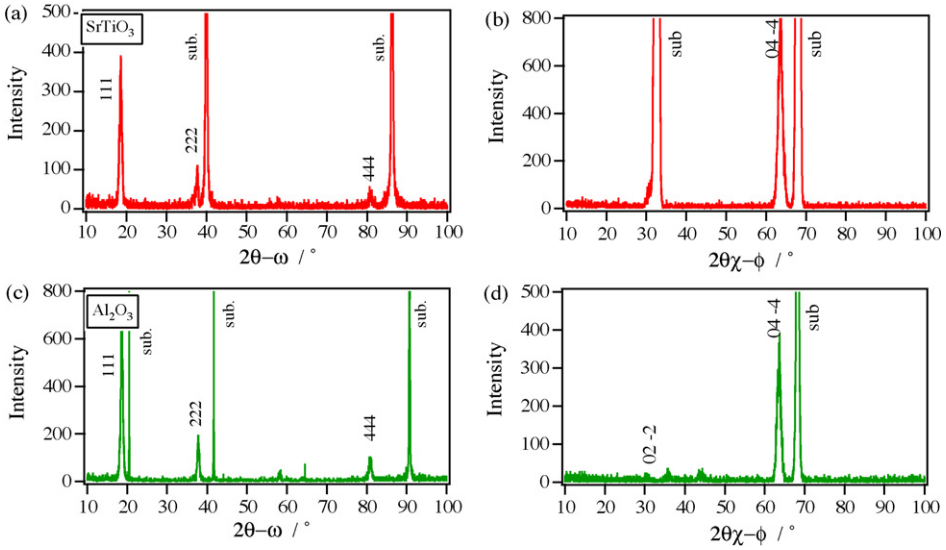

Fig. 1. X-ray diffraction patterns of $LiMn_2O_4$ thin films. Out-of-plane (a) and in-plane (b) XRD patterns for $LiMn_2O_4$/$SrTiO_3$(1 1 1) and out-of-plane (c) and in-plane (d) patterns for $LiMn_2O_4$/Al_2O_3(0 0 1).

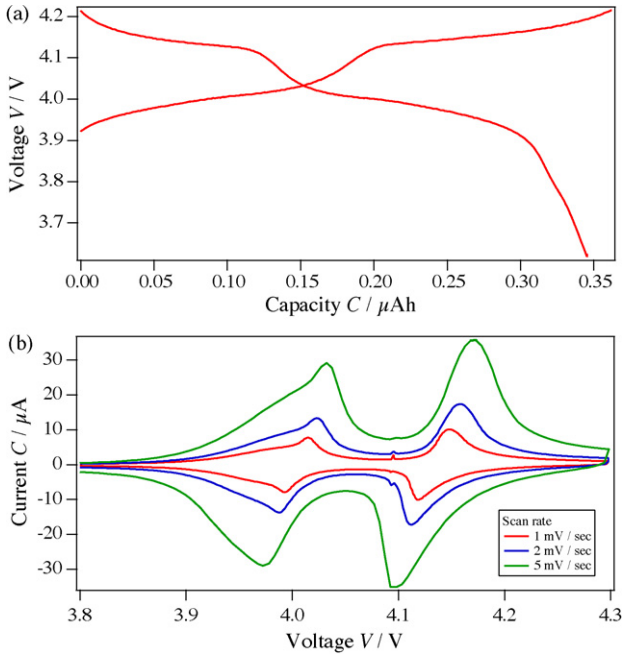

Fig. 2. Charge–discharge curves (a) and CV curves at various scan rate (b) of $LiMn_2O_4$ thin film deposited on Au polycrystalline substrate.

group [15]. This fast reaction would be brought by short lithium ion diffusion length owing to very thin film thickness. In Fig. 3(a) and (b), charge–discharge curves and CV curves for $LiMn_2O_4$ epitaxial film on Al_2O_3 substrate ($LiMn_2O_4/Al_2O_3$) were shown. The charge–discharge curves of $LiMn_2O_4/Al_2O_3$ epitaxial film were much different from those of $LiMn_2O_4$/Au. $LiMn_2O_4/Al_2O_3$ film showed only single plateau in 4 V region. In CV curves (Fig. 3(b)), a broad peak around 4.0 V and a slight shoulder around 4.15 V were observed. The scan rate dependence of peak separations was summarized in Table 1. The scan rate dependence of separation for the peak around 4.2 V is smaller than that of the peak around 4.0 V, while scan rate dependence at the $LiMn_2O_4$/Au electrode was almost the same between couples of two peaks. These results suggest that the CV peak at higher voltage for $LiMn_2O_4/Al_2O_3$ electrode would be assigned to other electrochemical reaction, perhaps electrolyte solvent decomposition. It should be noted that the scan rate dependence of peak separations for $LiMn_2O_4/Al_2O_3$ is larger than that for $LiMn_2O_4$/Au. Epitaxial thin film electrode is expected to show fast charge transfer performance owing to its excellent structure, i.e., low grain boundary effect, ordered single orientation and very flat surface. In spite of these superior characteristics, charge transfer at $LiMn_2O_4/Al_2O_3$ epitaxial film electrode was not fast as $LiMn_2O_4$/Au film. At the present stage, the accurate reason is unknown. But, the electric contact to the film would be an important factor for the fast charge transfer. For the

Table 1
CV peak separation of $LiMn_2O_4$/Au film and $LiMn_2O_4/Al_2O_3$ epitaxial film at the various scan rates.

Substrates	Peak separation (V)			
	Polycrystalline Au		Al_2O_3(0 0 1) single crystal	
Peak position	4.0 V	4.1 V	4.0 V	4.15 V
Scan rate (mV s^{-1})				
1.0	0.018	0.023	0.05	0.05
2.0	0.029	0.033	–	–
5.0	0.048	0.054	0.18	0.13
10.0	–	–	0.23	0.15

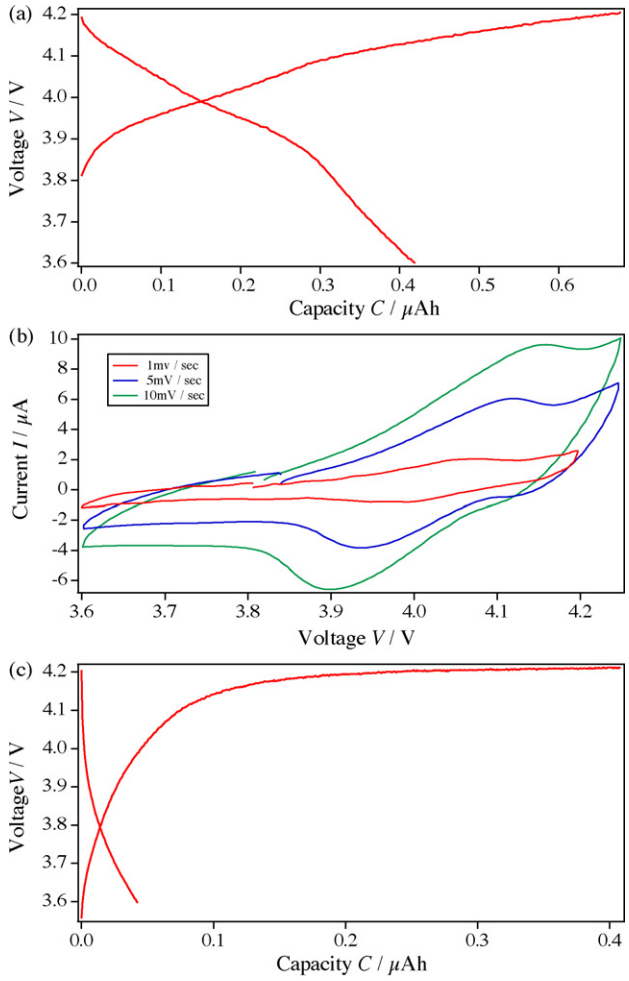

Fig. 3. Electrochemical property of $LiMn_2O_4$ epitaxial thin films. Charge–discharge curves (a), CV curves at various scan rates (b) of $LiMn_2O_4$ thin film deposited on Al_2O_3 (0 0 1) substrate, and charge–discharge curves of $LiMn_2O_4$ thin film deposited on $SrTiO_3$:Nb (1 1 1) substrate (c).

electric contact to $LiMn_2O_4/Al_2O_3$ film, we evaporated Au at the four edges of the film. This "partial" and weak contact compared with $LiMn_2O_4$/Au film, may make the lithium ion diffusion length longer.

The charge–discharge curves for $LiMn_2O_4$/STO epitaxial film were shown in Fig. 3(c). The discharge plateau voltage for $LiMn_2O_4$/STO (3.6–3.8 V) was lower than that for $LiMn_2O_4/Al_2O_3$ (3.8–4.1 V) and discharge capacity was also smaller. This difference would be caused by the interaction between the thin films and the substrates, because any serious difference was not found in crystal structure measured by the thin film XRD (Fig. 1). This interaction between the substrate and epitaxial film could be categorized to the electrical interaction at the film/substrate interface or the formation of a new inactive interface between the film and the substrate. For the detailed discussion, further investigation of the interface is necessary.

As was seen in Fig. 3, charge–discharge curves of $LiMn_2O_4/Al_2O_3$ showed single plateau. The two-stage plateau of bulk $LiMn_2O_4$ is reported to be caused by the phase transition of $Li_xMn_2O_4$ [16]. At the hetero-epitaxial interface, the substrate and the deposited material are connected directly by the chemical bond sharing the oxygen atoms at the interface surface. This direct connection and the induced strain may suppress the phase transition of $LiMn_2O_4$ epitaxial film.

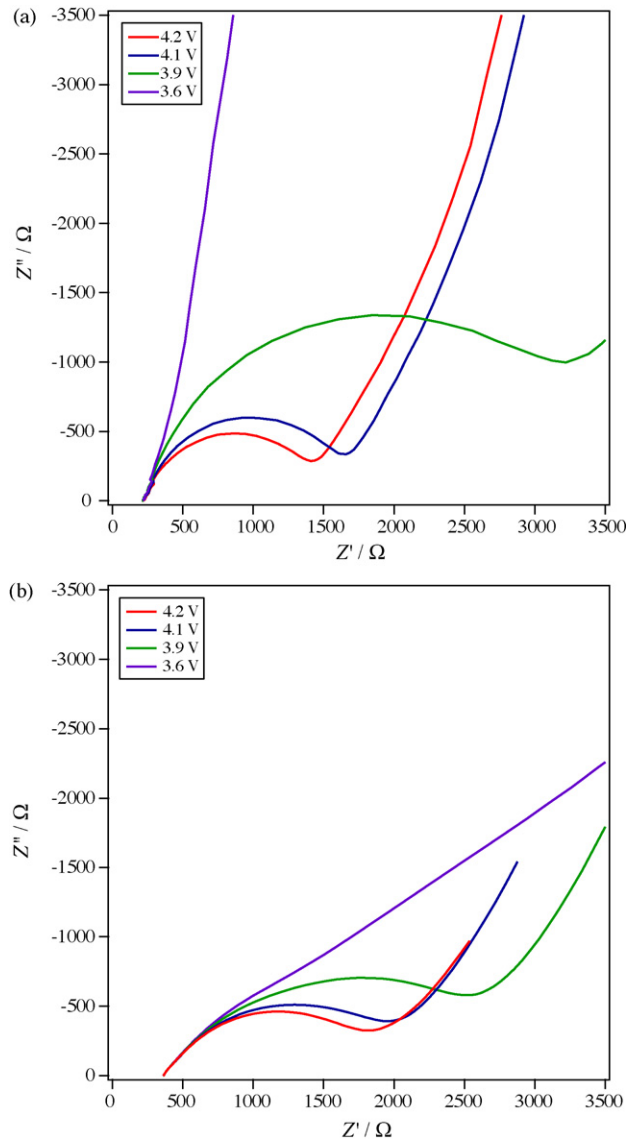

Fig. 4. Nyquist plots of (a) $LiMn_2O_4$ thin film deposited on Au polycrystalline substrate and (b) $LiMn_2O_4$ epitaxial film on Al_2O_3 (0 0 1) substrate at various potentials.

In Fig. 4, Nyquist plots of $LiMn_2O_4/Al_2O_3$ and $LiMn_2O_4$/Au films at given potentials are shown. These two films showed similar behavior. At the potential of 3.6 V, only blocking electrode behavior was observed. Above 3.9 V, one semi-circle appeared in the higher frequency region and this semi-circle became smaller with the increase in the voltage. This tendency, which agrees with the report by Yamada et al. [14] for $LiMn_2O_4$ film synthesized by PLD method, indicates the lithium ion (de-)intercalation is proceeding at the $LiMn_2O_4/Al_2O_3$ epitaxial film.

3.3. *Absorption spectrum measurement of $LiMn_2O_4/Al_2O_3$ epitaxial film during lithium ion intercalation*

Using the $LiMn_2O_4/Al_2O_3$ epitaxial film, that has high transparency for the weak light scattering at the surface of crystal, UV–visible absorption measurement of $LiMn_2O_4$ during lithium (de-)intercalation was carried out. The structure of the cell for absorption measurement is shown in Fig. 5. To obtain the path for light, the substrate holder has a square window and there also is a quartz glass window at the cell wall opposite side to the substrate

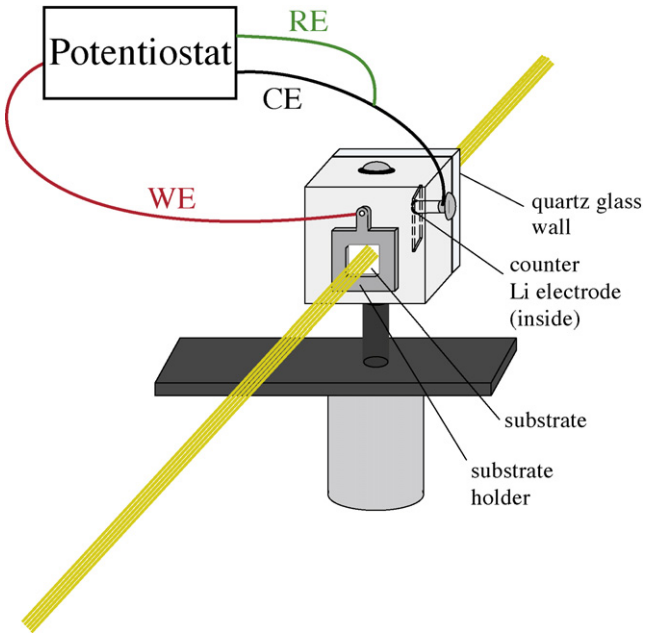

Fig. 5. Schematic description of the absorption spectrum measurement cell structure for the epitaxial thin film during lithium (de-)intercalation.

holder. The counter Li metal electrode is located at the side wall out of the light path. To confirm the cell performance, absorption spectrum measurement of WO_3 thin film, that is a famous material turning its color during the intercalation, was carried out. In Fig. 6, the absorption spectrum changes of WO_3/Al_2O_3 film during lithium intercalation are shown. On discharging (intercatation), the absorption in the UV region decreased monotonously with absorption increase in the visible region. Finally, the film color turned from no color to blue. The absorption spectrum of WO_3/Al_2O_3 film changed reversibly by the lithium (de-)intercalation. Fig. 7 shows the absorption and its derivative spectra of $LiMn_2O_4/Al_2O_3$ epitaxial film. One strong and two weak absorption were observed at the region below 500 nm, around 600 nm, and around 700 nm. These peaks were assigned to the band transition of $LiMn_2O_4$, transition from Mn t_{2g} to upper Mn e_g orbital and from Mn t_{2g} to lower Mn e_g orbital, respectively [17], and the positions of absorption agreed with the literature. The absorption spectra of $LiMn_2O_4/Al_2O_3$ epitaxial film at various voltages are shown in Fig. 8. During the lithium

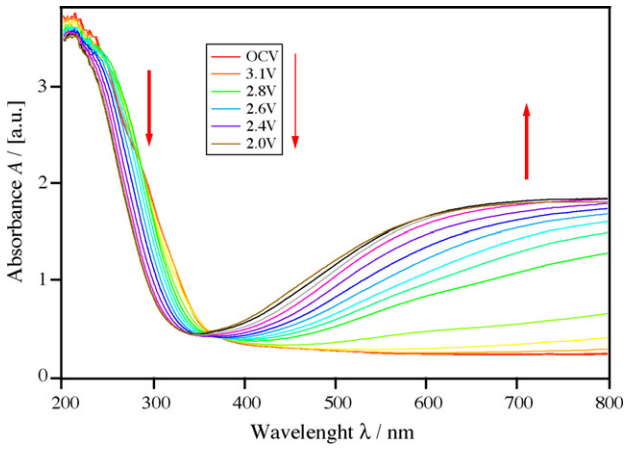

Fig. 6. Absorption spectra of WO_3 thin film on Al_2O_3 at various voltages during lithium intercalation.

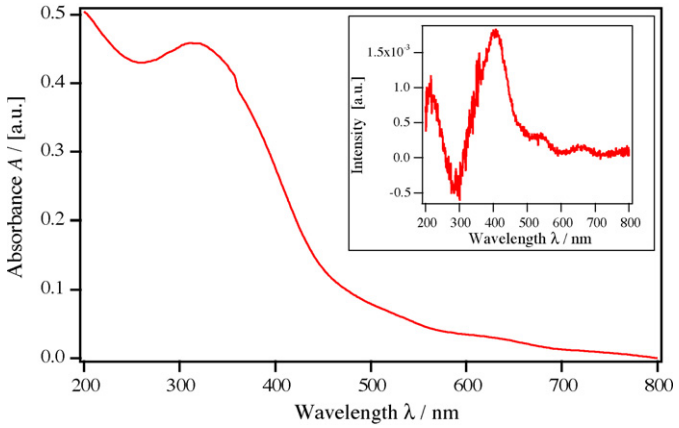

Fig. 7. Absorption spectrum and derivative spectrum (inset) of $LiMn_2O_4$ film on Al_2O_3.

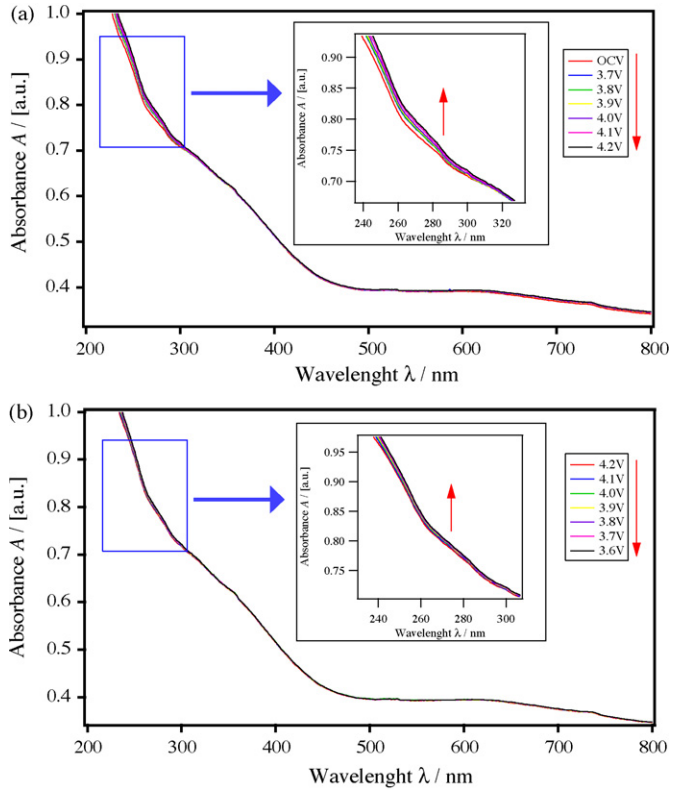

Fig. 8. Absorption spectrum changes of $LiMn_2O_4$ film on Al_2O_3 at various voltages on (a) charging and (b) discharging.

ion (de-)intercalation (Fig. 8(a)), the spectrum scarcely changed except for the slight increase in the UV region. During the lithium intercalation (Fig. 8(b)), the absorption in the UV region continued increasing. This monotonous absorption increase in the UV region was caused by the electrolyte solvent decomposition and that was confirmed by absorption measurement of electrolyte solution after the charge–discharge cycles.

The result that the absorption spectrum of $LiMn_2O_4/Al_2O_3$ epitaxial film showed no change during the lithium (de-)intercalation, suggests that the *d* orbitals and *d*-electrons of $LiMn_2O_4$ does not concern with the redox reaction in 4 V region lithium intercalation. Uchimoto et al. [18] measured the XANES spectra of $Li_xMn_2O_4$ ($0.1 \leq x \leq 2.2$) and reported that no shift of XANES spectra was observed for the specimens $0.1 \leq x \leq 1.0$. They explained this phenomenon as follows. A hole is introduced into the O *2p* orbital instead of drawing electrons from e_g orbital of Mn for the 4 V region $LiMn_2O_4$ charging. The results of the absorption spectrum measurement in this study may support this redox reaction mechanism.

4. Conclusion

In this paper, we have demonstrated that the electrochemical property of $LiMn_2O_4$ epitaxial thin film is influenced by the substrates those are chemically connected to the thin films. For the further development of epitaxial film electrode system, the optimization of substrate materials on the basis of the interface interactions would be necessary.

References

[1] A. Yamada, M. Yonemura, Y. Takei, N. Sonoyama, R. Kanno, Electrochem. Solid-State Lett. 8 (2005) A55–A58.
[2] M. Yonemura, A. Yamada, Y. Takei, N. Sonoyama, R. Kanno, J. Electrochem. Soc. 151 (2004) A1352–A1356.
[3] M. Okubo, E. Hosono, J. Kim, M. Enomoto, N. Kojima, T. Kudo, H. Zhou, I. Honma, J. Am. Chem. Soc. 129 (2007) 7444–7452.
[4] T. Abe, F. Sagane, M. Ohtsuka, Y. Iriyama, Z. Ogumi, J. Electrochem. Soc. 152 (2005) A2151–A2154.
[5] D. Aurbach, K. Gamolsky, B. Markovsky, G. Salitra, Y. Gofer, U. Heider, R. Oesten, M. Schmidt, J. Electrochem. Soc. 147 (2000) 1322–1331.
[6] M. Balasubramanian, H.S. Lee, X. Sun, X.Q. Yang, A.R. Moodenbaugh, J. McBreen, D.A. Fischer, Z. Fu, Electrochem. Solid-State Lett. 5 (2002) A22–A25.
[7] K. Edstroem, T. Gustafsson, J.O. Thomas, Electrochim. Acta 50 (2004) 397–403.
[8] J. Lei, L. Li, R. Kostecki, R. Muller, F. McLarnon, J. Electrochem. Soc. 152 (2005) A774–A777.
[9] Y. Wang, X. Guo, S. Greenbaum, J. Liu, K. Amine, Electrochem. Solid-State Lett. 4 (2001) A68–A70.
[10] M. Hirayama, K. Sakamoto, T. Hiraide, D. Mori, A. Yamada, R. Kanno, N. Sonoyama, K. Tamura, J. Mizuki, Electrochim. Acta 53 (2007) 871–881.
[11] M. Hirayama, N. Sonoyama, T. Abe, M. Minoura, M. Ito, D. Mori, A. Yamada, R. Kanno, T. Terashima, M. Takano, K. Tamura, J. Mizuki, J. Power Sources 168 (2007) 493–500.
[12] M. Hirayama, N. Sonoyama, M. Ito, M. Minoura, D. Mori, A. Yamada, K. Tamura, J. Mizuki, R. Kanno, J. Electrochem. Soc. 154 (2007) A1065–A1072.
[13] A. Rougier, K.A. Striebel, S.J. Wen, E.J. Cairns, J. Electrochem. Soc. 145 (1998) 2975–2980.
[14] I. Yamada, T. Abe, Y. Iriyama, Z. Ogumi, Electrochem. Commun. 5 (2003) 502–505.
[15] S.B. Tang, M.O. Lai, L. Lu, Electrochim. Acta 52 (2006) 1161–1168.
[16] S. Mukerjee, T.R. Thurston, N.M. Jisrawi, X.Q. Yang, J. McBreen, M.L. Daroux, X.K. Xing, J. Electrochem. Soc. 145 (1998) 466–472.
[17] K. Kushida, K. Kuriyama, Appl. Phys. Lett. 76 (16) (2000) 2238–2240.
[18] Y. Uchimoto, T. Yao, Mater. Integr. 12 (3) (1999) 43–48.